Fish and Shellfish Immunology 84 (2019) 223–232

Contents lists available at ScienceDirect

Fish and Shellfish Immunology

journal homepage: www.elsevier.com/locate/fsi

Full length article

Identification and characterization of a carboxypeptidase N1 from red lip mullet (*Liza haematocheila*); revealing its immune relevance

N.C.N. Perera[a], G.I. Godahewa[a], Sumi Jung[a], Myoung-Jin Kim[a], Bo-Hye Nam[b], Jehee Lee[a,*]

[a] Department of Marine Life Sciences & Fish Vaccine Research Center, Jeju National University, Jeju Self-Governing Province, 63243, Republic of Korea
[b] Biotechnology Research Division, National Institute of Fisheries Science, 408-1 Sirang-ri, Gijang-up, Gijang-gun, Busan, 46083, Republic of Korea

ARTICLE INFO

Keywords:
Carboxypeptidase N1
Complement component
Immunity
Lactococcus garviae
NO assay

ABSTRACT

Complement system orchestrates the innate and adaptive immunity *via* the activation, recruitment, and regulation of immune molecules to destroy pathogens. However, regulation of the complement is essential to avoid injuries to the autologous tissues. The present study unveils the characteristic features of an important complement component, anaphylatoxin inactivator from red lip mullet at its molecular and functional level. Mullet carboxypeptidase N1 (MuCPN1) cDNA sequence possessed an open reading frame of 1347 bp, which encoded a protein of 449 amino acids with a predicted molecular weight of 51 kDa. *In silico* analysis discovered two domains of PM14-Zn carboxypeptidase and a C-terminal domain of M14 N/E carboxypeptidase, two zinc-binding signature motifs, and an N-glycosylation site in the MuCPN1 sequence. Homology analysis revealed that most of the residues in the sequence are conserved among the other selected homologs. Phylogeny analysis showed that MuCPN1 closely cladded with the *Maylandia zebra* CPN1 and clustered together with the teleostean counterparts. A challenge experiment showed modulated expression of MuCPN1 upon polyinosinic:polycytidylic acid and *Lactococcus garviae* in head kidney, spleen, gill, and liver tissues. The highest upregulation of MuCPN1 was observed 24 h post infection against poly I:C in each tissue. Moreover, the highest relative expressions upon *L. garviae* challenge were observed at 24 h post infection in head kidney tissue and 48 h post infection in spleen, gill, and liver tissues. MuCPN1 transfected cells triggered a 2.2-fold increase of nitric oxide (NO) production upon LPS stimulation compared to the un-transfected controls suggesting that MuCPN1 is an active protease which releases arginine from complement C3a, C4a, and C5a. These results have driven certain way towards enhancing the understanding of immune role of MuCPN1 in the complement defense mechanism of red lip mullet.

1. Introduction

The immune system is a complex network which is essential to regulate the homeostasis of a host organism. It is equipped with numerous effector mechanisms involved in the detection and prosecution of pathogens, toxicants, and allergens, which threaten host viability. Interestingly, the immune system evolves continuously to be more specific, efficient, and more complex to combat a broad range of pathogens as well as to clear a broad range of toxic and allergenic substances. Immunity is mainly divided into two parts: innate and adaptive, according to the rapidity and the specificity of the responses toward pathogenic infections [1].

The complement system is a highly sophisticated defense mechanism, which plays key roles in both innate and adaptive immunity [2,3]. It consists of plasma proteins that can be directly activated against pathogens. Activation of the complement system can be initiated in three pathways, the alternative, lectin, and classical. Alternative and lectin pathways are involved in the innate immune system, where the classical pathway induces the adaptive immune system [4–8]. A chain of reactions starts when the complement system is activated by identification of a pathogenic surface. Potent inflammatory mediators like anaphylatoxins are released to combat pathogens while other complement molecules opsonize the pathogenic surfaces to facilitate the lysis [9]. The C3a, C4a, and C5a proteins cause the anaphylatoxin activities of smooth muscle contraction, increase in blood capillary permeability, chemotaxis, and degranulation at the site of pathogen infection [10,11]. However, the complement activities must be regulated by the system to protect the host cells and organs from

* Corresponding author. Marine Molecular Genetics Lab, Department of Marine Life Sciences, Jeju National University, Jeju Self-Governing Province, 63243, Republic of Korea.
E-mail address: jehee@jejunu.ac.kr (J. Lee).

https://doi.org/10.1016/j.fsi.2018.10.010
Received 24 May 2018; Received in revised form 29 September 2018; Accepted 5 October 2018
Available online 06 October 2018
1050-4648/

bystander damage as autologous injury. In the complement system several regulators may be involved in the process of inhibition of lysis, cleavage of anaphylatoxins, and decaying the accelerating activity for C3 convertases to avoid such injuries [12,13]. Carboxypeptidases are known to cleave the carboxyl-terminal arginine and lysine from peptides especially in the complement system [10,14,15]. Carboxypeptidase N (CPN) is an important regulator of the complement system involved in the regulation of complement activities.

CPN, also known as arginine carboxypeptidase, kininase I, anaphylatoxin inactivator, is a plasma zinc metalloprotease, and it consists of two small subunits (CPN1) and two large subunits (CPN2) [10]. These enzymatically active subunits protect the protein from degradation by the complement system. CPN1 is mostly accountable for the regulation of the biological activities of C3a, C4a, and C5a in the complement system, thus called an anaphylatoxin inactivator. It has been reported that CPN is mostly expressed in the liver and secreted to the bloodstream [10,16].

Additionally, diverse diseases have also been reported with defects in the carboxypeptidases [17]. A remarkable decrease in the level of carboxypeptidase N was observed in patients with chronic urticarial or angioedema [18]. Moreover, mice with destructed CPN1 active subunits showed an increase in susceptibility towards the C5a anaphylatoxin-mediated shock [19]. CPN1 was found to be expressed in early embryonic development and no total deficiency of CPN1 has yet been reported [20]. Taken together, this suggests that complete deficiency of CPN1 might be fatal, as it is an essential molecule for the regulation of host biological functions [19].

Red lip mullet is one of the economically important aqua-crop in Republic of Korea. Though, the prevalence of infectious diseases causes negative impacts on the quality and quantity of its production. Control of the infectious pathogens through the innate immunity of red lip mullet may be a crucial factor to reduce the production losses. This paper attempts to investigate the characteristic features of a teleostean carboxypeptidase N1 from red lip mullet (*Liza haematocheila*), and evaluates its homology and evolutionary relationships with known homologs. Immune responses of mullet CPN1 (MuCPN1) were evaluated upon polyinosinic:polycytidylic acid (poly I:C) and *Lactococcus garviae* challenges. Moreover, functional behavior of MuCPN1 was assessed through a nitric oxide assay.

2. Methodology

2.1. Mullet cDNA database construction and MuCPN1 sequence identification

The transcriptome database of mullet was constructed by *de novo* assembly using the IsoSeq method. Briefly, the total RNA was extracted and purified from kidney, spleen, head kidney, gill, skin, liver, intestine, stomach, heart, eye, brain, and blood tissues of five mullet using the QIAzol lysis reagent and cleaned the purified RNA using RNeasy Mini Kit (Qiagen, USA) according to the guidelines of manufacturer. The extracted RNA was then sent to Insilicogen, Korea and first strand cDNA was synthesized using the Clontech SMRTer PCR cDNA Synthesis Kit. Then, cDNA were fractioned based on the fragment size and converted into SMRTbell templates for sequencing on PacBio platform. Subsequently, base calling, adapter trimming and barcode removing was carried out to identify the full length reads based on the 5′ terminal cDNA primers and 3′ terminal polyA tail signals. Then, assembly classification removes the polyA/T tails, primers and classified the full-length and non-full-length transcripts. Generated transcript sequences were subjected to gene annotation using Blast2Go software. The constructed mullet transcriptome database was used to obtain the CPN1 homolog sequence. The corresponding sequence was analyzed using the BLAST program at the National Center for Biotechnology Information (NCBI) (http://blast.ncbi.nlm.nih.gov/Blast.cgi) to corroborate the MuCPN1 homolog. Finally, the MuCPN1 cDNA sequence was deposited in the GenBank with the accession No: MH373662.

2.2. Bioinformatics analysis of MuCPN1

An open reading frame (ORF), amino acid sequence, molecular mass, and theoretical isoelectric point was derived using the DNAssist (ver. 2.2) program and protparam tool (https://web.expasy.org/protparam/). Characteristic domains and motifs were identified through homology comparison in the conserved domain database (CDD) at NCBI, Motif Scan (http://myhits.isb-sib.ch/cgi-bin/motif_scan), and ExPASy PROSITE (http://prosite.expasy.org/) databases. Putative signal peptides were predicted using the SignalP (http://www.cbs.dtu.dk/services/SignalP/) server. The secondary structure of MuCPN1 protein was discovered by the Predict Protein tool (http://ppopen.informatik.tu-muenchen.de/) and ITASSER online server. Multiple sequence alignment was performed by Clustal Omega (https://www.ebi.ac.uk/Tools/msa/clustalo/), and a phylogenetic tree was reconstructed by using the Neighbor-Joining (NJ) method at MEGA (ver. 6.0). Folding pattern of the MuCPN1 and its degree of folding was predicted by the Fold index©, online bioinformatics tool (http://bip.weizmann.ac.il/fldbin/findex) [21]. Moreover, tertiary structure was predicted by SWISS-MODEL (https://swissmodel.expasy.org/) using the human CPN1 (PDB: 2nsm.1, crystal structure of the human carboxypeptidase N catalytic chain) as a template.

2.3. Experimental fish rearing

Healthy red lip mullets with an average body weight of 100 g were acquired from Sangdeok fishery in Hadong, Korea for the transcriptional analysis of the MuCPN1. Fish were temporally fed and reared in 400 L laboratory aquarium tanks (salinity: 34 ± 1%, pH 7.6 ± 0.5 at 20 ± 1 °C for) with a density of 30 fish per tank for one week prior to experimental manipulation. Disease spread and other stress factors were eliminated during the experiment. All the animal experiments were reviewed and permitted by the Animal Care and Use Committee of Jeju National University.

2.4. Tissue distribution analysis

In order to determine the spatial expression profile of MuCPN1, five randomly selected, pre-acclimatized mullet fish were anesthetized (MS-222; 40 mg/L) and twelve different tissues were collected aseptically. Initially, blood was collected by sterile syringes coated with heparin sodium salt (USB, USA), and peripheral blood cells were isolated by instantaneous centrifugation at 3000 × *g* for 10 min at 4 °C. Other tissues including liver, head kidney, spleen, kidney, gill, brain, heart, muscle, skin, intestine, and stomach were excised and snap-frozen in liquid nitrogen and stored.

2.5. Immune challenge experiment

An immune stimulation was carried out by delivering the intraperitoneal injection (100 μL) of poly I:C (1.5 μg/g, Sigma, USA) and *L. garvieae* (1×10^3 CFU/μL) into healthy mullets. Poly I:C and *L. garvieae* were suspended in 1 × phosphate buffered saline (PBS), hence PBS injection was delivered as a control treatment. In order to determine the immune modulation of MuCPN1 upon viral mimic and bacterial immune stimulant injections, five mullets from each treatment were randomly anesthetized (MS-222; 40 mg/L) and dissected at 0-, 6-, 24-, 48- or 72 h post-injection (p.i.). The spleen, head kidney, gill, and liver tissues were collected and snap-frozen in liquid nitrogen and stored.

2.6. Total RNA isolation and first strand cDNA synthesis

Tissues from five individuals were equally homogenized and

Table 1
Primers used in present study.

Description	Primer Sequence
MuCPN1-qPCR forward	5′-ACAAGTCAAGAGACCCTCGCATCAG-3′
MuCPN1-qPCR reverse	5′—CCTGCATGCCTTTGGACAGAGAGTA-3′
MuEF1α-qPCR forward	5′—CCCTGGTCAGATCAGTGCTGGTTAT-3′
MuEF1α-qPCR reverse	5′-AGCGTCGCCAGACTTTAGGGATTT-3′
MuCPN1-cloning forward	5′-GAGAGAaagcttATGCATCAGAGGTGGACTCTCCTC-3′
MuCPN1- cloning reverse	5′-GAGAGAgatatcTCATCTGGGGCCGAGCTTTAAATTG-3′

subjected for the total RNA extraction using QIAzol lysis reagent (Qiagen, Germany). These were cleaned-up with an RNeasy spin column (Qiagen, Germany) and RNA quality was examined on 1.5% agarose gel electrophoresis. The concentration and purity of total RNA was determined at 260 nm in a μDrop Plate Reader (Thermo Scientific USA). First-strand cDNA was synthesized using 2.5 μg of isolated RNA according to the manufacturer's guidelines using PrimeScript™ II 1st strand cDNA Synthesis Kit (TaKaRa, Japan). Synthesized cDNA was diluted 40-fold in nuclease-free water and stored at −80 °C until used in qPCR analysis.

2.7. Quantitative real time PCR (qPCR) analysis

A pair of gene specific primers (Table 1) was used to explore the mRNA expression patterns of MuCPN1. Mullet elongation factor 1 alpha (EF1α) (Accession No; MH017208) was used as an internal control gene [22]. The qPCR was conducted using a Thermal Cycler Dice™ TP950 (TaKaRa, Japan).

Triplicated PCR reactions were performed in a 10 μL reaction volume containing 3 μL of cDNA template, 5 μL of 2 × TaKaRa Ex Taq™ SYBR premix, 0.4 μL of each of the forward and reverse primers (10 pmoL/μL) and 1.2 μL of H_2O. The thermal cycling outline used in this study was as follows: primary denaturation at 95 °C for 10 s, followed by 45 cycles of denaturation, annealing and extension at 95 °C for 5 s, 58 °C for 10 s, and 72 °C for 20 s, respectively. Final dissociation of MuCPN1 and MuEF1α genes expressions were implemented at 95 °C for 15 s, 60 °C for 30 s, and 95 °C for 15 s.

Relative transcriptions of MuCPN1 were quantified according to the Livak method [23]. To examine the spatial expression profile of the MuCPN1, values were calibrated using the intestine transcript level. The transcript level of the MuCPN1 at 0 h p.i. was used for the calibration in the temporal expression profile analysis, followed by relative MuCPN1 mRNA expression was determined by comparison with PBS injected controls at the corresponding post injection times. The significant up-regulations of MuCPN1 in head kidney, spleen, gill, and liver were compared with the respective PBS-injected controls and the untreated (0 h) control value was set as the basal transcriptional level.

2.8. Construction of the plasmids, cell culture, and nitric oxide assay

The full length CDS of MuCPN1 with a 1350 bp was amplified using the gene specific primers (Table 1) and cloned into pcDNA3.1(+) vector (Invitrogen™, USA) containing restriction recognition sites of *Hin*dIII and *Eco*RV. A positive clone harboring the MuCPN1 CDS was confirmed through sequencing (Macrogen, Korea) and designated as MuCPN1-pcDNA3.1(+). In order to determine the effects of CPN1 on the nitric oxide (NO) production, murine macrophage RAW264.7 cells were used to overexpress MuCPN1. Briefly, a monolayer of RAW264.7 cells (1×10^5 cells/well) was seeded in 6-well plates in complete Dulbecco's Modified Eagle's Medium (DMEM). The cells with 80–90% confluence were transiently transfected with MuCPN1-pcDNA3.1(+) and empty vector, pcDNA3.1(+) by using X-tremeGENE 9 DNA transfection reagent (Roche, Germany). The transfected cells were then stimulated with LPS at a concentration of 100 ng/mL 24 h post transfection. Then the cells were incubated for another 12 h at 37 °C. Supernatant was collected and transferred to a 96-well plate treated with Griess reagent (1% sulganilamide and 0.1 naphthylenediamine dihydrochloride in 2.5% of phosphoric acid) and incubated for 10 min at room temperature, 25 °C. Finally, the absorbance was measured at 540 nm in a microplate reader (Multiskan GO, Thermo Scientific USA). Reactions were performed in triplicates.

2.9. Statistical analysis

All experiments including transcriptional analysis and the activity of MuCPN1 were repeated three times. Results were expressed as mean ± standard deviation (SD) of the triplicates. The data were subjected to one-way analysis of variance (ANOVA) followed by Duncan's Multiple Range Post-Hoc Test using the SPSS 16.0 program (USA). The p values less than 0.05 were considered as statistically different ($P < 0.005$). Additionally, web-based Graphpad statistical software (http://graphpad.com/quickcalcs/ttest1.cfm) was used to estimate the significant differences in the activity assay by two-tailed *t*-test.

3. Results

3.1. Identification and the domain topology of MuCPN1 cDNA sequence

Full-length cDNA sequence of the carboxypeptidase N1 was isolated from the constructed mullet cDNA database and designated as MuCPN1 (GenBank accession NO: MH373662). The cDNA sequence of MuCPN1 possessed a 5′ un-translated region (UTR) of 133 bp, an open reading frame (ORF) of 1347 bp, and a 3′ UTR of 312 bp (Fig. 1). The predicted ORF of MuCPN1 encoded a protein of 449 amino acids with a predicted molecular mass of 51 kDa. According to the protparam tool, MuCPN1 had a theoretical isoelectric point of 6.6 and the protein is stable with an instability index of 28.15. Moreover, it is predicted to be an extracellular protein in the mullet with a prediction accuracy of 93%. The results obtained through the signal peptide analysis suggested that MuCPN1 possessed a signal peptide at the N-terminus. The NetNGlyc web tool confirmed the presence of an N-glycosylation site at 436–438 aa. *In silico* analysis unveiled two domains including, PM14-Zn carboxypeptidase and a C-terminal domain of M14 N/E carboxypeptidase in the MuCPN1 sequence. Moreover, two zinc-binding signature motifs were found in the MuCPN1 sequence. Zinc binding sites (H^{91}, E^{94}, and H^{221}) and the other active sites (H^{91}, E^{94}, R^{156}, N^{161}, R^{162}, H^{221}, G^{222}, N^{228}, D^{232}, G^{285}, Y^{289}, L^{291}, and E^{311}) were located among the domains and the signatures of the MuCPN1. Additionally, ten α-helices and sixteen β-strands linked with coils were observed in the secondary structure of MuCPN1.

3.2. Alignments and homology analysis of CPN1

Pairwise analysis with known CPN1 orthologs indicated that MuCPN1 shared more than 85% identity with other teleosts and more than 65% identity with mammalian counterparts (Fig. 2). The highest identity towards MuCPN1 was shared by two CPN1 orthologs from *Oplegnathus fasciatus* and *Stegastes partitus* (~94%). However, the sequence similarities among these CPN1 orthologs were 97.3% and 97.1%, respectively.

Most of the residues of MuCPN1 were highly conserved among fish orthologs where a substantial degree of conservation can be observed among the characteristics domains and the signatures of the selected CPN1 orthologs (Fig. 3). However, a highly variable nature was observed at the N terminus and C terminus of the CPN1 orthologs.

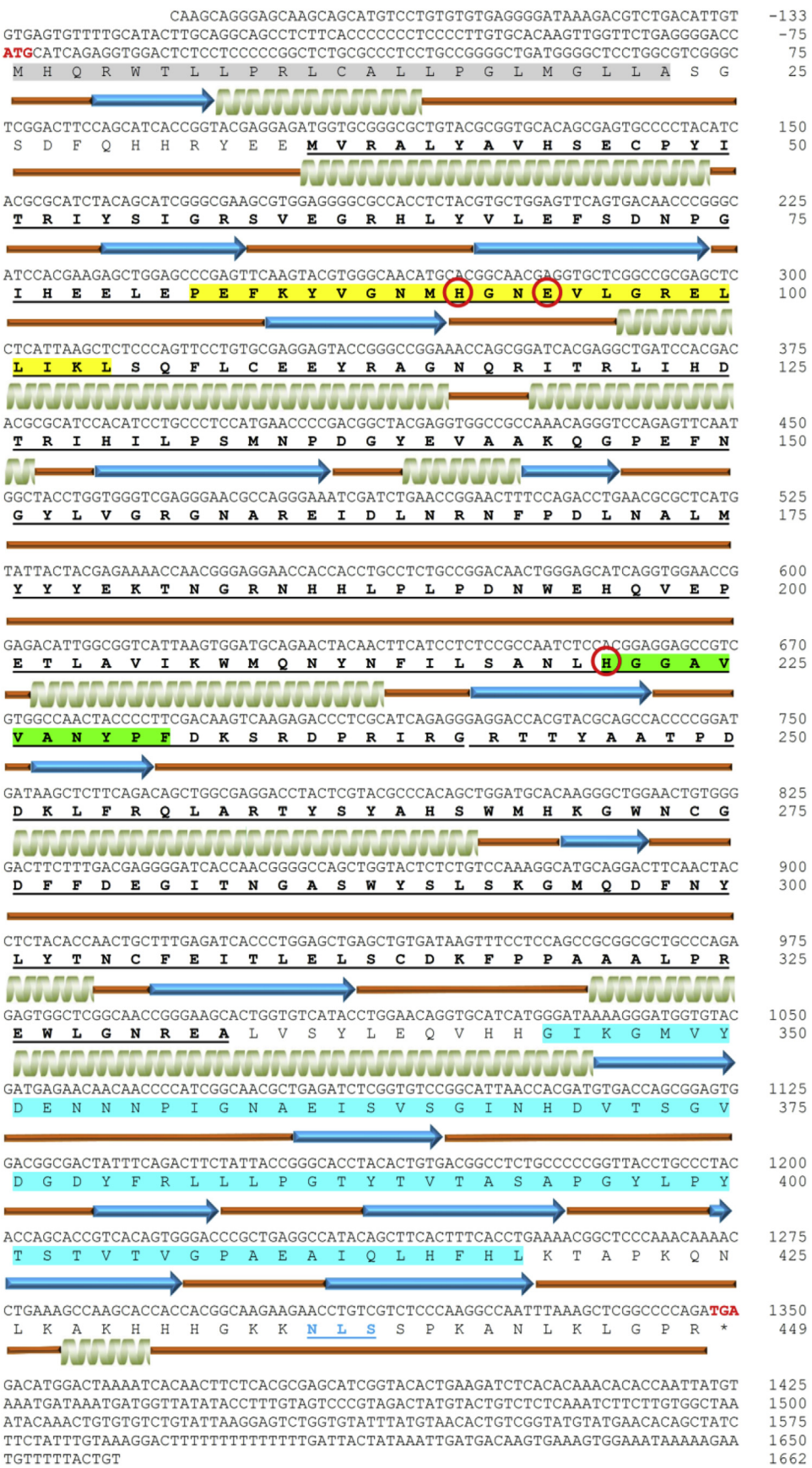

Fig. 1. Analysis figure of MuCPN1. The nucleotide sequence (upper) and the deduced amino acid sequence (lower) are numbered. The start codon (ATG) and stop codon (TAG) are red and bold. Conserved domains are denoted by different symbols within the coding region. The signal peptide is shaded in grey. PM14-Zn carboxypeptidase domain was highlighted as underlined in black and C-terminal domain M14 N/E carboxypeptidase domain was highlighted in sky blue. Zinc-binding signature 1 and zinc-binding signature 2 were highlighted in yellow and green, respectively. Zinc binding sites are denoted by red circles, and the N-glycosylation sites were denoted in blue colored underlined letters. Secondary structural features of MuCPN1 are presented below each amino acid sequence: green wave - a-helix; blue arrow - b-strand; orange line - coil and Tissue distribution analysis revealed a ubiquitous expression in all examined tissues with an intense expression in spleen tissue. (For interpretation of the references to color in this figure legend, the reader is referred to the Web version of this article.)

CPN1			*L. haematocheilus*	*O. fasciatus*	*S. partitus*	*S. dumerili*	*D. labrax*	*L. crocea*	*P. olivaceus*	*O. niloticus*	*M. zebra*	*P. formosa*	*H. sapiens*	*X. tropicalis*	*M. musculus*	*B. taurus*	*R. norvegicus*
Scientific Name	**Accession No**		**Identity%**														
Liza haematocheila	MH373662	**Similarity%**		94.00	94.00	92.20	92.00	91.80	91.20	91.10	90.90	89.10	67.60	66.90	65.70	65.60	65.00
Oplegnathus fasciatus	AIZ96978		97.30		96.70	95.50	96.90	96.00	94.00	93.10	93.10	89.10	67.20	66.40	65.60	65.20	64.50
Stegastes partitus	XP_008290452		97.10	98.20		95.10	95.50	94.40	93.60	93.80	93.80	89.70	67.00	66.20	65.20	64.80	64.30
Seriola dumerili	XP_022599049		96.70	98.00	97.30		94.00	93.50	94.30	91.50	91.50	89.10	66.70	66.50	64.80	65.20	63.90
Dicentrarchus labrax	CBN81456		96.00	97.80	96.90	96.90		94.60	92.70	92.20	92.40	89.10	66.50	67.00	64.90	64.50	63.90
Larimichthys crocea	XP_010740379		96.40	97.80	96.90	96.90	96.90		92.50	91.50	91.50	89.50	66.50	65.90	65.10	65.00	64.20
Paralichthys olivaceus	XP_019938894		95.40	96.90	96.20	96.70	95.80	96.70		91.20	90.90	88.30	65.70	65.40	64.70	63.80	63.90
Oreochromis niloticus	XP_003441899		96.00	97.10	96.70	96.20	96.00	96.90	95.80		98.70	87.90	67.40	64.80	65.60	65.90	64.90
Maylandia zebra	XP_004567539		95.50	96.70	96.20	95.80	95.50	96.40	95.40	99.60		87.70	67.40	64.80	65.60	65.90	65.20
Poecilia formosa	XP_007574356		94.70	94.00	94.40	93.80	93.80	94.90	93.60	93.80	93.30		65.20	65.90	65.00	64.50	63.90
Homo sapiens	NP_001299		79.00	79.70	79.70	80.60	78.80	78.80	80.30	80.10	80.10	78.60		68.10	83.40	86.20	82.80
Xenopus tropicalis	NP_001017266		81.70	80.60	80.60	80.20	80.80	80.40	79.60	80.60	80.60	80.00	81.00		67.60	67.20	67.40
Mus musculus	NP_109628		77.90	78.80	77.90	77.90	77.70	77.90	78.10	78.30	78.30	77.70	91.30	78.10		82.70	96.50
Bos taurus	DAA14819		78.10	78.80	79.20	79.70	78.10	77.90	79.40	80.10	80.10	78.60	92.20	81.20	89.80		81.60
Rattus norvegicus	NP_445978		77.50	77.50	76.80	77.20	76.40	77.20	77.20	77.70	77.90	76.40	91.30	77.90	98.00	88.70	

Fig. 2. Homology analysis of MuCPN1 with identity and similarity percentage of its known orthologs.

Additionally, Zn binding sites were highly conserved among the other homologs selected in the present analysis.

3.3. Relative position of MuCPN1 in phylogeny analysis

A phylogenetic tree was constructed using the amino acid sequences of CPN1 orthologs from different lineages (Fig. 4). The un-rooted phylogeny showed two main divisions, higher vertebrates and lower vertebrates, of CPN1 members. All the CPN1 orthologs clustered with each other to form individual subgroups based on taxonomy. MuCPN1 was cladded in the teleost cluster and shared a strong evolutionary relationship with other fish orthologs.

3.4. Folding prediction and homology modeling of 3D structure of MuCPN1

Hydrophobicity and the absolute net charge of the amino acids can be used to predict the foldability of the known amino acid sequence using Foldindex©. Extensive folded regions were observed in the graphical illustration of the folding predictions in MuCPN1, rock bream CPN1, zebrafish CPN1, and human CPN1 (Fig. 5A). Five disordered regions composed of 119 aa residues were observed in the MuCPN1 (Fig. 5B). Similar results were shown by the *D. rerio* CPN1 compared to 7 disordered regions shown by the *H. sapiens* CPN1 counterpart. The three-dimensional structure of MuCPN1 was visualized with the homology modeling tools (Fig. 5C). Similar folding patterns were observed in both MuCPN1 and human CPN1. The well folded structure of MuCPN1 was displayed with 10 α-helices and 16 β strands in the predicted diagram. The Zn binding sites of the MuCPN1 were centralized in the three-dimensional structure.

3.5. Tissue specific transcriptional analysis of MuCPN1

Physiological characteristic features were studied *via* a tissue specific transcriptional analysis with healthy juveniles. Ubiquitous expression was detected in all the selected tissues, including intestine, brain, kidney, heart, gill, skin, stomach, muscle, blood, head kidney, liver, and spleen (Fig. 6). However, the magnitudes of these expressions were different from each tissue. Increased expression of MuCPN1 was observed in the spleen (~30.08-fold) followed by liver (~21.13-fold), and head kidney (~17.57-fold). Here, fold value of intestine tissue was set as the basal value for the qPCR analysis.

3.6. Immune responses of MuCPN1 upon immune stimuli

Immune responsive role of MuCPN1 was studied through an immune challenge using immune stimulants of poly I:C and *L. garvieae*. Modulated mRNA expression profiles were observed in head kidney, spleen, gill, and liver tissues (Fig. 7). The highest upregulation of MuCPN1 against poly I:C was observed at 24 h post infection in all the examined tissues. The highest expression of MuCPN1 against *L. garvieae* was detected at 48 h post infection in spleen, gill, and liver tissues. However, in head kidney tissue, increased expression of MuCPN1 was observed at 24 h post infection against *L. garvieae*. Though the MuCPN1 was modulated upon poly I:C and *L. garvieae*, the pattern of expression profiles were differed in all four tissues.

3.7. Nitric oxide production assay

In order to investigate NO production upon MuCPN1-generated arginine, NO production was assayed with MuCPN1-pcDNA3.1(+) transfected murine macrophage RAW 264.7 cells. Elevated NO production was observed compared to the control treatments (Fig. 8). In comparison with untransfected and pcDNA3.1(+) transfected control cells, the MuCPN1-pcDNA3.1(+) transfected cells triggered a 2.2-fold increase in NO production upon LPS (1 μg/mL) stimulation.

4. Discussion

Emerging diseases have become a principal constraint towards sustainable aquaculture production. A variety of stress factors including high density, poor nutrition, and microbial quality in the cultured water increase infections by opportunistic pathogens and lead to devastating production losses [24]. In order to design effective disease prevention measures, it is important to study the host-pathogen interactions and the host defense systems at the molecular level. Present study explores an important immune component that plays key roles in both innate and adaptive immunity. The complement pathway is a cascade of plasma proteins that interact with pathogens to protect the host. However, over expression of complement system destruct the tissue homeostasis by anaphylatoxin-induced effects [25–27]. Interestingly, the activity of the anaphylatoxins including C3a, C4a, and C5a was regulated by CPN1 *via* cleaving the C-terminal Arg residue of C3a, C4a, and C5a [13,15,28]. In the present study, the CPN1 gene was identified and characterized from red lip mullet to discover its involvement in the mullet immune defense system.

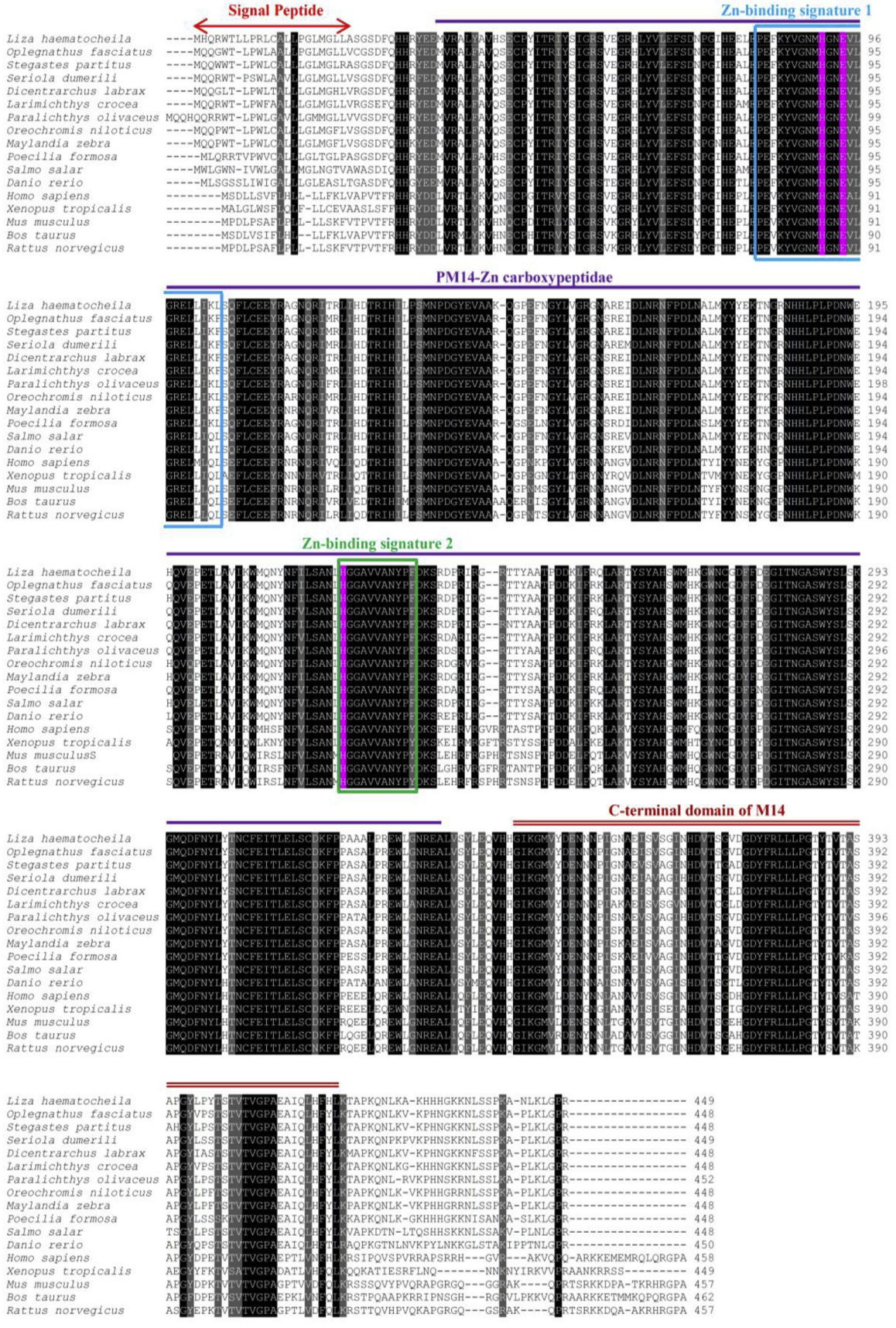

Fig. 3. Multiple alignment of MuCPN1. Residues identically conserved are shaded in black and residues similarly conserved in all selected animals are shaded in grey. Zinc binding sites are shaded in pink. (For interpretation of the references to color in this figure legend, the reader is referred to the Web version of this article.)

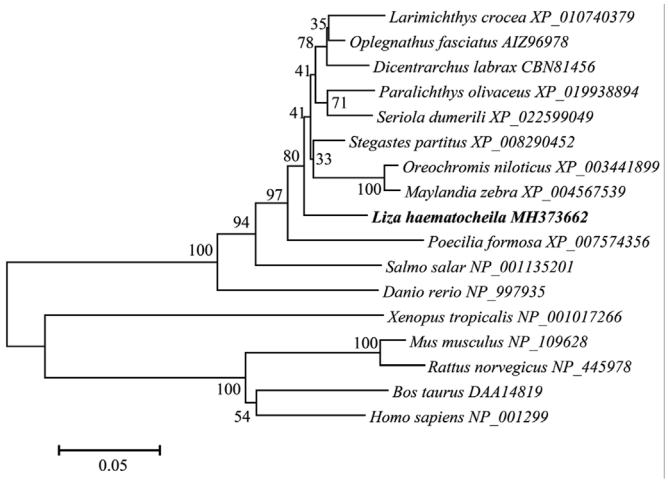

Fig. 4. Phylogenetic analysis of MuCPN1. Representative CPN1 orthologs from selected species were aligned with MuCPN1 using MEGA5. The bootstrap confidence values derived from 5000 replications were mentioned in the nodes.

The putative MuCPN1 gene, identified from the mullet cDNA sequence database showed a significant identity with the number of amino acids and predicted molecular mass of CPN1s of other teleosts [29] and mammalian counterparts [11]. Moreover, a highly conserved domain architecture (PM14-Zn carboxypeptidase and C-terminal domain of M14 N/E carboxypeptidase) including other signature motifs (zinc-binding signature motifs) and active sites further verified that MuCPN1 is indeed a CPN1 homolog (Fig. 3). These conserved domains are important for hydrolyzation of the c-terminal amino acids from the target peptide where the zinc binding sites are suggested to provide the electro-statistic stabilization for the negatively charged intermediates [30]. Additionally, other active sites are important for substrate binding catalysis. According to homology analysis, these identified residues may play critical roles in structure or function and thus may have been preserved throughout the evolution. However, variations and substitutions of specific amino acid residues may reflect a specific position of MuCPN1 during evolution. Collectively, resulted higher evolutionary conservation signifies that CPN1 proteins are likely to have important biological functions in mammalian and teleostean counterparts. Evolutionary relationships resulted by phylogenetic analysis further suggests potential commonalities of MuCPN1 with teleost counterparts, thus it exclusively has a piscine origin.

It is generally assumed that the function of a protein is linked with its structure. Folding predictions suggested MuCPN1 was well structured through the whole protein with a high level of folding. Interestingly CPN is a tetramer with two heterodimers comprised of two main subunits [20,31]. These two subunits are very tightly associated with each other and extremely stable in the blood stream [10]. Moreover, numerous interactions of CPN were reported including binding to fibrinogen and fibrin [32], membrane interactions [31] and the interactions with complement pathway molecules [33]. Non-folding proteins and non-folding regions of particular proteins were more susceptible to rapid evolution than the structured proteins due to their low stability [34]. Additionally, intrinsically disordered regions facilitate the regulation of a large number of protein interactions [35,36]. Therefore, the intrinsically disordered regions of the MuCPN1 sequence may be important for its protein-protein interactions and its biological function as an anaphylatoxin inactivator. The three-dimensional structure of MuCPN1 also evidenced for having a well-structured folding regions through the sequence which may apparently be attributed to the interactions of the CPN1 protein in mullet. The numbers of the helices and β-strands were more or less similar to those of humans [31] and other fish counterparts [29] revealing its structural integrity. Moreover, closely occupied active sites and zinc binding sites might be crucial in MuCPN1 interactions and for the substrate recognition.

The potential physiological role of MuCPN1 was studied through its mRNA expression profile in major tissues, including immune associated tissues of healthy mullets. A ubiquitous expression of MuCPN1 further emphasized that it may be an essential molecule for the defense mechanism and basal expression might be necessary for the survival of the mullet. Expression of MuCPN1 was highest in the spleen followed by the liver (Fig. 6). Spleen and liver are the most important tissues that remove a majority of bacteria from the bloodstream [37]. Additionally, the spleen is a phagocytic filter which plays critical roles in protecting against infections [38,39]. Macrophages are responsible for recognizing the pathogens that cross the epithelial barrier [40,41]. Moreover, macrophages express mediators and regulators of anaphilatoxins that can be activated by the complement pathway which could secrete cytokines and chemokines [42]. Interestingly, a large number of macrophages can be found in both spleen and liver tissues [43–46]. Additionally, carboxypeptidases are synthesized in the liver and secreted into the blood where concentration is high [10,31]. These findings could suggest that high expression of MuCPN1 in both the spleen and liver are necessary for its biological function in the mullet. Moreover, these results concur with previous studies which have shown that CPN1 mRNA expression was high in liver and kidney tissues [29].

The complement system has been recognized as a central system in both innate and adaptive immunity as it involves protecting the host against pathogens *via* bridging the innate and adaptive immune responses [2,47]. Therefore, to understand the transcriptional modulations as immune-related responses against viral and bacterial infections, a time course challenged experiment was conducted with mullet. Highlighted modulations of MuCPN1 against immune stimuli reveal its involvement in the innate immune responses (Fig. 7). As a model of viral infection, polyI:C, a synthetic double stranded RNA [48,49], was used in the challenged experiment. Moreover, *Lactococcosis* sp. prevalent on mullet resulted in serious economic losses in Taiwan [50]. Therefore, we selected *L. garviae* as a gram positive coccal pathogen [51] for our bacterial challenged experiment. The modulated expression pattern revealed that MuCPN1 may be involved in generating immune responses during infection. However, the modulation pattern of MuCPN1 showed little difference in each tissue towards different immune stimulants, suggesting the immune response of MuCPN1 may be tissue specific. Modulated expression profiles of rock bream CPN1 was also been reported against lipopolysaccharide, *Streptococcus iniae*, *Edwardisell tarda*, rock bream irido virus and poly I:C in liver tissue [29]. The different modulation patterns of MuCPN1 and rock bream CPN1 suggest that the expression of CPN1 is species specific as well.

Carboxypeptidases cleave arginine from the C terminal of peptidases. These arginine residues are suggested to induce NO production under inflammatory conditions [52]. Our present study proved that MuCPN1 transfected cells increase the production of nitric oxide in LPS treated murine macrophage RAW 264.7 cells. Wu and Morris stated that Arg is essential during the development and wound healing [53]. Moreover, arginine generated NO plays important roles in diverse processes, including immune responses, adhesion of platelets and leucocytes and neurotransmission [54,55]. On the other hand, present results suggest that MuCPN1 could hydrolyze the C terminal amino acid of the complement anaphylatoxin molecules and may regulate the complement system. Taken together, it can be suggested that MuCPN1 is an important complement molecule in the mullet immune system which mediates the immune responses against pathogenic infection.

5. Conclusions

Summing up the entire study; full-length cDNA sequence for MuCPN1 was identified and characterized as the second study in the teleosts. The outcome of homology analysis showed MuCPN1 was well positioned with known counterparts including other vertebrates. Phylogeny analysis further verified that MuCPN1 has evolved from a

(A)

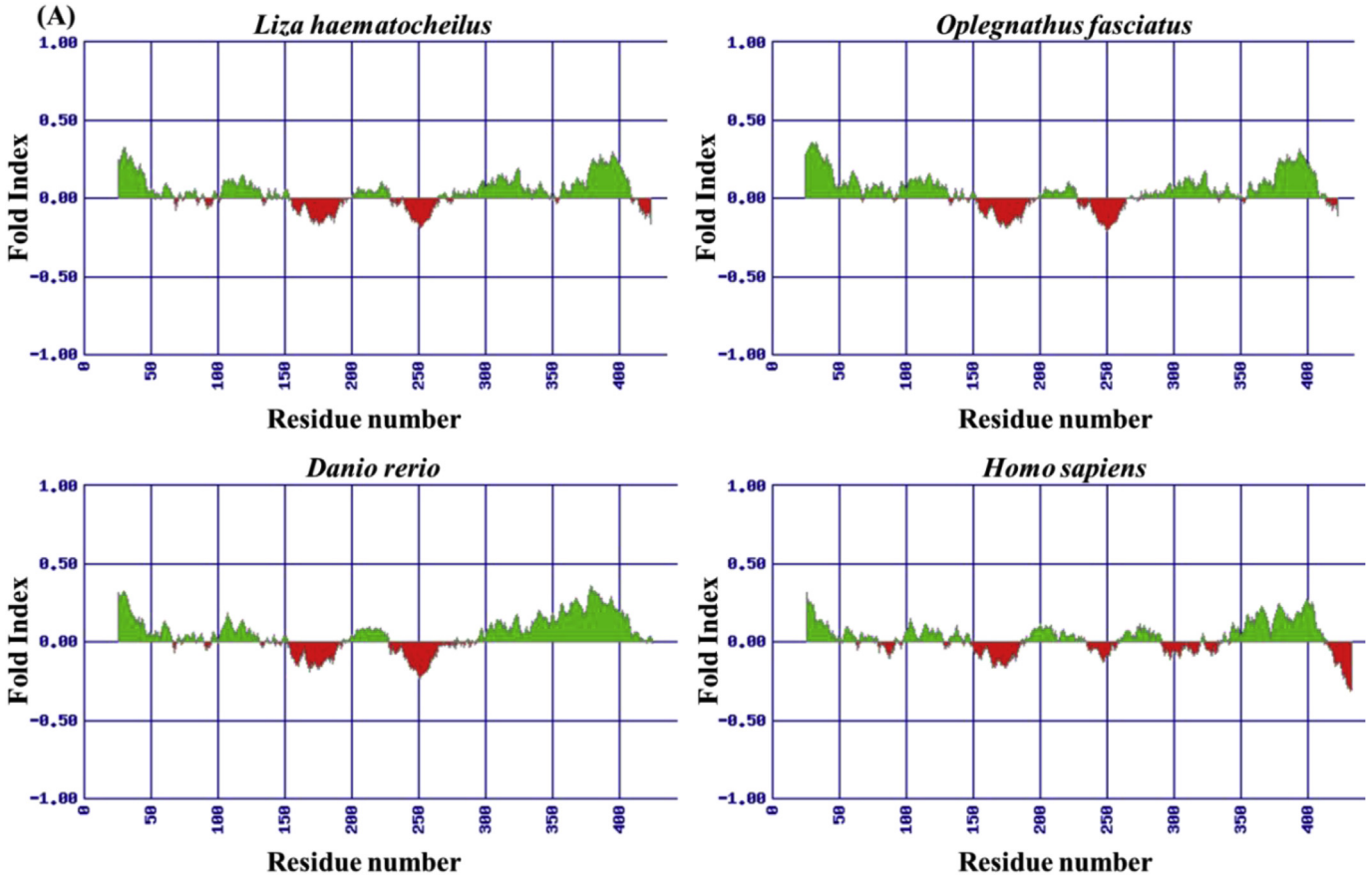

(B)

Organism	Total length of the protein (aa)	No. of disordered regions	No. of disordered residues (aa)	Percentage of the disordered residues
Liza haematocheilus	449	5	119	26.50
Oplegnathus fasciatus	448	3	112	25.00
Danio rerio	450	5	125	27.78
Homo sapiens	458	7	163	35.58

(C) (D)

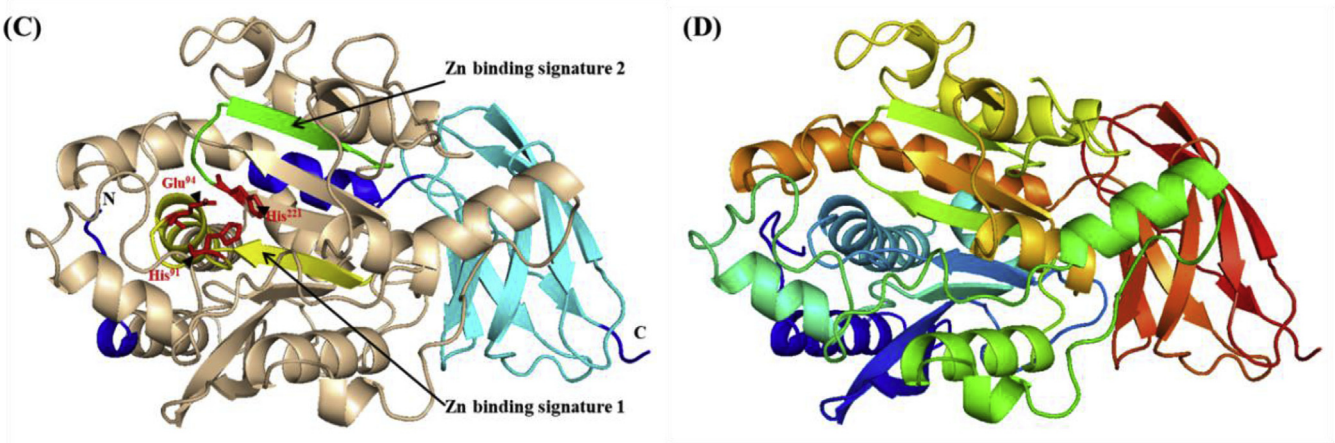

Fig. 5. Graphical representation of folding predictions (A), Fold index (B) of CPN1 counterparts. Intrinsically folded regions are in light green where intrinsically unfolded regions are in red color. Tertiary structure analysis of MuCPN1 (C) and human CPN1 (D). MuCPN1 PM14-Zn carboxypeptidase is in wheat color, and Zn binding sites are in red. C-terminal domain of M14 is in sky blue. (For interpretation of the references to color in this figure legend, the reader is referred to the Web version of this article.)

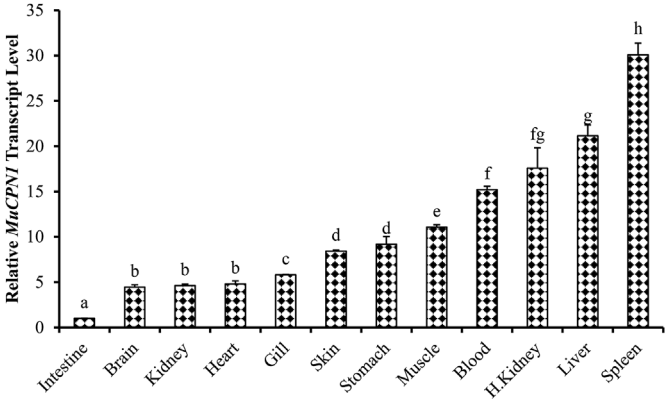

Fig. 6. Constitutive mRNA expression of *MuCPN1* in tissues of healthy mullets. The calculation was performed using the Livak method and the values were calibrated against the mRNA level in the intestine. The mRNA levels of different tissues were compared by one-way analysis of variance (ANOVA) and Duncan's Multiple Range Post-Hoc Test. Data with different letters are significantly different ($P < 0.05$).

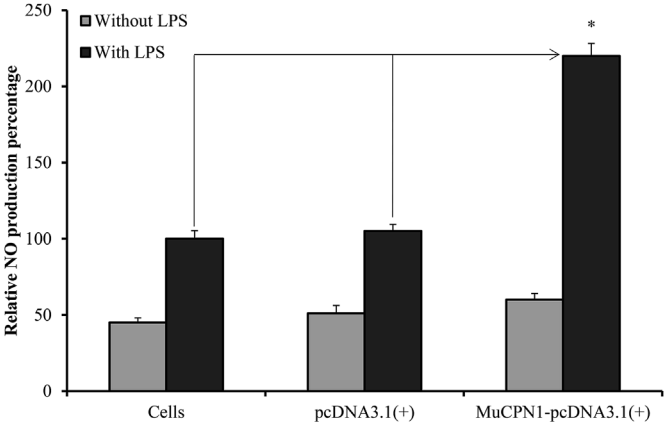

Fig. 8. Relative Nitric oxide (NO) production by MuCPN1 in the presence and absence of LPS. The absorbance was measured at OD_{540} and the assay was conducted in triplicates. Significant difference compared to the control cells are indicated with an asterisk (*, $P < 0.005$).

common ancestor of vertebrate orthologs. Ubiquitous expression of MuCPN1 among all the selected tissues unveiled the importance of the MuCPN1 in mullet physiology. The transcriptional responsiveness upon bacterial and viral stimuli through relevant immune challenges was illustrated. Finally, it was proved that MuCPN1 could enhance the nitric oxide production during the inflammation process in the murine macrophage RAW 264.7 cells. On the basis of these promising results it can be stated, as a stepping stone for future studies regarding the complement components and their involvement in the innate and adaptive immune defense of fish.

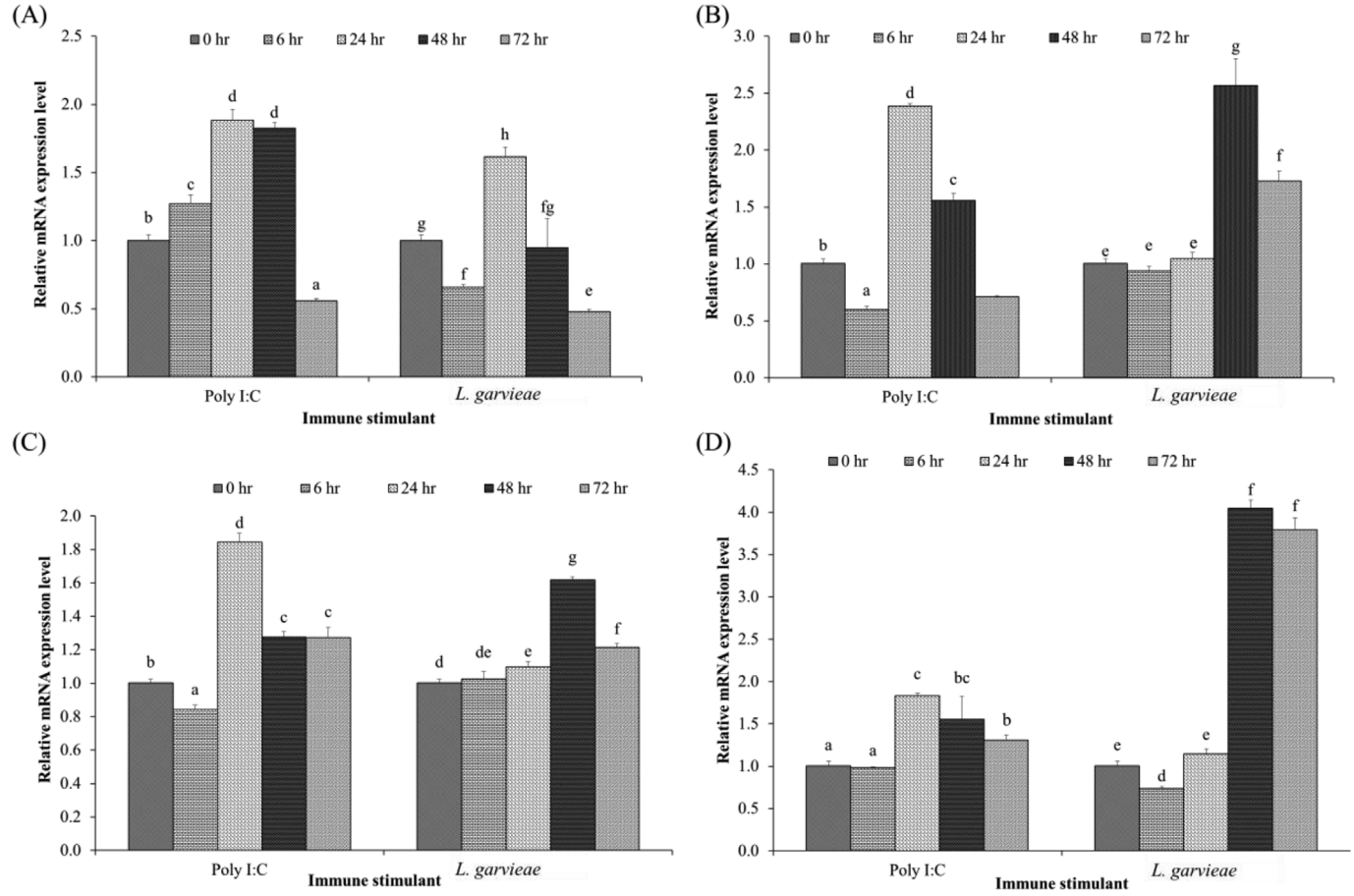

Fig. 7. Transcriptional levels of *MuCPN1* in immune challenged head kidney (A), spleen (B), gill (C), and liver (D) tissues against *in vivo* challenge with poly I:C and *L. garviae*. In each group gene expression at 0 h was set as 1. The mRNA levels in different time points were compared by one-way analysis of variance (ANOVA) and Duncan's Multiple Range Post-Hoc Test. The mean ± SD (n = 3) were represented with the vertical bars. Data with different letters are significantly different ($P < 0.05$).

Acknowledgment

This research was a part of the project titled 'Fish Vaccine Research Center', funded by the Ministry of Oceans and Fisheries, Korea and supported by a grant from Marine Biotechnology Program (20180430, Genome Analysis of Marine and Fisheries Organisms and Development of functional Application) Funded by Ministry of Oceans and Fisheries, Korea.

References

[1] K.L. Rock, J.J. Lai, H. Kono, Innate and adaptive immune responses to cell death, Immunol. Rev. 243 (1) (2011) 191–205.
[2] J.R. Dunkelberger, W.C. Song, Complement and its role in innate and adaptive immune responses, Cell Res. 20 (1) (2010) 34–50.
[3] H. Molina, V.M. Holers, B. Li, Y. Fung, S. Mariathasan, J. Goellner, J. Strauss-Schoenberger, R.W. Karr, D.D. Chaplin, Markedly impaired humoral immune response in mice deficient in complement receptors 1 and 2, Proc. Natl. Acad. Sci. U. S. A. 93 (8) (1996) 3357–3361.
[4] Y.M. Ali, N.J. Lynch, K.S. Haleem, T. Fujita, Y. Endo, S. Hansen, U. Holmskov, K. Takahashi, G.L. Stahl, T. Dudler, U.V. Girija, R. Wallis, A. Kadioglu, C.M. Stover, P.W. Andrew, W.J. Schwaeble, The lectin pathway of complement activation is a critical component of the innate immune response to pneumococcal infection, PLoS Pathog. 8 (7) (2012) e1002793.
[5] T. Fujita, Evolution of the lectin-complement pathway and its role in innate immunity, Nat. Rev. Immunol. 2 (5) (2002) 346–353.
[6] C. Suankratay, C. Mold, Y. Zhang, L.A. Potempa, T.F. Lint, H. Gewurz, Complement regulation in innate immunity and the acute-phase response: inhibition of mannan-binding lectin-initiated complement cytolysis by C-reactive protein (CRP), Clin. Exp. Immunol. 113 (3) (1998) 353–359.
[7] N.S. Merle, R. Noe, L. Halbwachs-Mecarelli, V. Fremeaux-Bacchi, L.T. Roumenina, Complement system Part II: role in immunity, Front. Immunol. 6 (2015) 257.
[8] C.H. Nielsen, E.M. Fischer, R.G. Leslie, The role of complement in the acquired immune response, Immunology 100 (1) (2000) 4–12.
[9] M.M. Markiewski, J.D. Lambris, The role of complement in inflammatory diseases from behind the scenes into the spotlight, Am. J. Pathol. 171 (3) (2007) 715–727.
[10] K.W. Matthews, S.L. Mueller-Ortiz, R.A. Wetsel, Carboxypeptidase N: a pleiotropic regulator of inflammation, Mol. Immunol. 40 (11) (2004) 785–793.
[11] Y. Levin, R.A. Skidgel, E.G. Erdos, Isolation and characterization of the subunits of human plasma carboxypeptidase N (kininase i), Proc. Natl. Acad. Sci. U. S. A. 79 (15) (1982) 4618–4622.
[12] M. Noris, G. Remuzzi, Overview of complement activation and regulation, Semin. Nephrol. 33 (6) (2013) 479–492.
[13] P.N. Nesargikar, B. Spiller, R. Chavez, The complement system: history, pathways, cascade and inhibitors, Eur. J. Microbiol. Immunol. (Bp) 2 (2) (2012) 103–111.
[14] J.M. Koomen, D. Li, L.C. Xiao, T.C. Liu, K.R. Coombes, J. Abbruzzese, R. Kobayashi, Direct tandem mass spectrometry reveals limitations in protein profiling experiments for plasma biomarker discovery, J. Proteome Res. 4 (3) (2005) 972–981.
[15] R.A. Skidgel, E.G. Erdos, Structure and function of human plasma carboxypeptidase N, the anaphylatoxin inactivator, Int. Immunopharm. 7 (14) (2007) 1888–1899.
[16] R.A. Skidgel, Basic carboxypeptidases: regulators of peptide hormone activity, Trends Pharmacol. Sci. 9 (8) (1988) 299–304.
[17] X. Hu, R.A. Wetsel, T.N. Ramos, S.L. Mueller-Ortiz, T.R. Schoeb, S.R. Barnum, Carboxypeptidase N-deficient mice present with polymorphic disease phenotypes on induction of experimental autoimmune encephalomyelitis, Immunobiology 219 (2) (2014) 104–108.
[18] K.P. Mathews, P.M. Pan, N.J. Gardner, T.E. Hugli, Familial carboxypeptidase N deficiency, Ann. Intern. Med. 93 (3) (1980) 443–445.
[19] S.L. Mueller-Ortiz, D. Wang, J.E. Morales, L. Li, J.Y. Chang, R.A. Wetsel, Targeted disruption of the gene encoding the murine small subunit of carboxypeptidase N (CPN1) causes susceptibility to C5a anaphylatoxin-mediated shock, J. Immunol. 182 (10) (2009) 6533–6539.
[20] K.W. Matthews, S.M. Drouin, C. Liu, J.F. Martin, R.A. Skidgel, R.A. Wetsel, Expression of the third complement component (C3) and carboxypeptidase N small subunit (CPN1) during mouse embryonic development, Dev. Comp. Immunol. 28 (6) (2004) 647–655.
[21] J. Prilusky, C.E. Felder, T. Zeev-Ben-Mordehai, E.H. Rydberg, O. Man, J.S. Beckmann, I. Silman, J.L. Sussman, FoldIndex: a simple tool to predict whether a given protein sequence is intrinsically unfolded, Bioinformatics 21 (16) (2005) 3435–3438.
[22] W. Meiqin, H. Lei, L. Wenshu, H. Naoshi, A. Junya, S. Kiyoshi, I. Yoshimasa, Z. Junsheng, H. Akihiko, Evaluation of environmental estrogenic activities in the Yangtze river estuary: utilization of vitellogenin production in red lip mullet, Aquacult. Sci. 59 (1) (2011) 65–73.
[23] K.J. Livak, T.D. Schmittgen, Analysis of relative gene expression data using real-time quantitative PCR and the 2(-Delta Delta C(T)) Method, Methods 25 (4) (2001) 402–408.
[24] A. Oliva-Teles, Nutrition and health of aquaculture fish, J. Fish. Dis. 35 (2) (2012) 83–108.
[25] J. Bjork, T.E. Hugli, G. Smedegard, Microvascular effects of anaphylatoxins C3a and C5a, J. Immunol. 134 (2) (1985) 1115–1119.
[26] M.M. Glovsky, T.E. Hugli, T. Ishizaka, L.M. Lichtenstein, B.W. Erickson, Anaphylatoxin-induced histamine release with human leukocytes: studies of C3a leukocyte binding and histamine release, J. Clin. Invest. 64 (3) (1979) 804–811.
[27] M.A. Flierl, D. Rittirsch, A.J. Chen, B.A. Nadeau, D.E. Day, J.V. Sarma, M.S. Huber-Lang, P.A. Ward, The complement anaphylatoxin C5a induces apoptosis in adrenomedullary cells during experimental sepsis, PloS One 3 (7) (2008) e2560.
[28] V.A. Bokisch, H.J. Muller-Eberhard, Anaphylatoxin inactivator of human plasma: its isolation and characterization as a carboxypeptidase, J. Clin. Invest. 49 (12) (1970) 2427–2436.
[29] G.I. Godahewa, W.D. Wickramaarachchi, I. Whang, S.D. Bathige, B.S. Lim, C.Y. Choi, M. De Zoysa, J.K. Noh, J. Lee, Two carboxypeptidase counterparts from rock bream (*Oplegnathus fasciatus*): molecular characterization, genomic arrangement and immune responses upon pathogenic stresses, Vet. Immunol. Immunopathol. 162 (3–4) (2014) 180–191.
[30] P. Aloy, V. Companys, J. Vendrell, F.X. Aviles, L.D. Fricker, M. Coll, F.X. Gomis-Ruth, The crystal structure of the inhibitor-complexed carboxypeptidase D domain II and the modeling of regulatory carboxypeptidases, J. Biol. Chem. 276 (19) (2001) 16177–16184.
[31] C. Keil, K. Maskos, M. Than, J.T. Hoopes, R. Huber, F. Tan, P.A. Deddish, E.G. Erdos, R.A. Skidgel, W. Bode, Crystal structure of the human carboxypeptidase N (kininase I) catalytic domain, J. Mol. Biol. 366 (2) (2007) 504–516.
[32] S. Talens, J.H. Lebbink, J.J. Malfliet, J.A. Demmers, S. Uitte de Willige, F.W. Leebeek, D.C. Rijken, Binding of carboxypeptidase N to fibrinogen and fibrin, Biochem. Biophys. Res. Commun. 427 (2) (2012) 421–425.
[33] N.S. Merle, S.E. Church, V. Fremeaux-Bacchi, L.T. Roumenina, Complement system Part I - molecular mechanisms of activation and regulation, Front. Immunol. 6 (2015) 262.
[34] A.K. Dunker, I. Silman, V.N. Uversky, J.L. Sussman, Function and structure of inherently disordered proteins, Curr. Opin. Struct. Biol. 18 (6) (2008) 756–764.
[35] P.E. Wright, H.J. Dyson, Intrinsically unstructured proteins: re-assessing the protein structure-function paradigm, J. Mol. Biol. 293 (2) (1999) 321–331.
[36] M.O. Collins, L. Yu, I. Campuzano, S.G. Grant, J.S. Choudhary, Phosphoproteomic analysis of the mouse brain cytosol reveals a predominance of protein phosphorylation in regions of intrinsic sequence disorder, Mol. Cell. Proteomics 7 (7) (2008) 1331–1348.
[37] J.F. Bohnsack, E.J. Brown, The role of the spleen in resistance to infection, Annu. Rev. Med. 37 (1986) 49–59.
[38] G.M. Fulop, D.B. McMillan, Phagocytosis in the spleen of the sunfish Lepomis spp, J. Morphol. 179 (2) (1984) 175–195.
[39] H.R. Shinefield, C.R. Steinberg, D. Kaye, Effect of splenectomy on the susceptibility of mice inoculated with *Diplococcus pneumoniae*, J. Exp. Med. 123 (5) (1966) 777–794.
[40] L. Helming, Inflammation: cell recruitment versus local proliferation, Curr. Biol. 21 (14) (2011) R548–R550.
[41] T.H. Mogensen, Pathogen recognition and inflammatory signaling in innate immune defenses, Clin. Microbiol. Rev. 22 (2) (2009) 240–273 (Table of Contents).
[42] M.A. Khan, A.M. Assiri, D.C. Broering, Complement and macrophage crosstalk during process of angiogenesis in tumor progression, J. Biomed. Sci. 22 (2015) 58.
[43] L.C. Davies, S.J. Jenkins, J.E. Allen, P.R. Taylor, Tissue-resident macrophages, Nat. Immunol. 14 (10) (2013) 986–995.
[44] F. Tacke, Targeting hepatic macrophages to treat liver diseases, J. Hepatol. 66 (6) (2017) 1300–1312.
[45] H. Kitani, M. Yoshioka, T. Takenouchi, M. Sato, N. Yamanaka, Characterization of the liver-macrophages isolated from a mixed primary culture of neonatal swine hepatocytes, Results Immunol. 4 (2014) 1–7.
[46] V. Bronte, M.J. Pittet, The spleen in local and systemic regulation of immunity, Immunity 39 (5) (2013) 806–818.
[47] M. Wills-Karp, Complement activation pathways: a bridge between innate and adaptive immune responses in asthma, Proc. Am. Thorac. Soc. 4 (3) (2007) 247–251.
[48] E. Vercammen, J. Staal, R. Beyaert, Sensing of viral infection and activation of innate immunity by toll-like receptor 3, Clin. Microbiol. Rev. 21 (1) (2008) 13–25.
[49] M.E. Fortier, S. Kent, H. Ashdown, S. Poole, P. Boksa, G.N. Luheshi, The viral mimic, polyinosinic:polycytidylic acid, induces fever in rats via an interleukin-1-dependent mechanism, Am. J. Physiol. Regul. Integr. Comp. Physiol. 287 (4) (2004) R759–R766.
[50] S.C. Chen, L.L. Liaw, H.Y. Su, C.Y. Wu, H.C. Chaung, Y.H. Tsai, K.L. Yang, Y.C. Chen, T.H. C, G.R. Lin, S.Y. Chen, Y.D. Lin, J.L. Lee, C.C. Lai, Y.J. Weng, S.Y. Chu, *Lactococcus garvieae*, a cause of disease in grey mullet, *Mugil cephalus* L., in Taiwan, J. Fish. Dis. 25 (2002) 727–732.
[51] O. Byadgi, Y.C. Chen, A.C. Barnes, M.A. Tsai, P.C. Wang, S.C. Chen, Transcriptome analysis of grey mullet (*Mugil cephalus*) after challenge with *Lactococcus garvieae*, Fish Shellfish Immunol. 58 (2016) 593–603.
[52] S. Moncada, E.A. Higgs, Molecular mechanisms and therapeutic strategies related to nitric oxide, Faseb. J. 9 (13) (1995) 1319–1330.
[53] G. Wu, S.M. Morris Jr., Arginine metabolism: nitric oxide and beyond, Biochem. J. 336 (Pt 1) (1998) 1–17.
[54] S. Moncada, Nitric oxide: discovery and impact on clinical medicine, J. R. Soc. Med. 92 (4) (1999) 164–169.
[55] D.S. Bredt, S.H. Snyder, Nitric oxide: a physiologic messenger molecule, Annu. Rev. Biochem. 63 (1994) 175–195.